International Journal of Automotive Technology, Vol. 16, No. 4, pp. 581−591 (2015)
DOI 10.1007/s12239−015−0059−5

pISSN 1229−9138/ eISSN 1976−3832

CONTROLLER DESIGN FOR A SEMI-TRACK AIR-CUSHION VEHICLE

C. MA, D. HE, D. XIE, F. YU* and Z. LUO

State Key Laboratory of Mechanical System and Vibration, School of Mechanical Engineering, Shanghai Jiao Tong University, Shanghai 200240, China

(Received 10 September 2013; Revised 12 September 2014; Accepted 8 December 2014)

ABSTRACT−To enhance the trafficability of semi-track air-cushion vehicle (STACV), a prototype is manufactured and a heirarchy controller is designed. The control objectives are, 1) to minimize the total power consumption; 2) to follow the driver's commands and maintain the body attitude; 3) to assign and realize the generalized forces. The controller is proposed by using carefully designed controller configuration, neural network, Model Predictive Control (MPC) method, hybrid generalized extremal optimization (HGEO), etc. Finally, the effectiveness of the proposed controller is verified by experiments under two typical operation conditions.

KEY WORDS : Semi-track air-cushion vehicle, Soft terrain, Optimal power consumption, Model predictive control, Body attitude control

1. INTRODUCTION

Because of transportation demand on soft and wet terrain, such as swamp, desert, oilfield and beach, many studies on air-cushion vehicles (Bertin, 1968; Bekker, 1969; Wong, 1973) have been carried out. Some hybrid vehicles combining air-cushion technology with different driving systems are studied to further improve the crossing-terrain ability (Luo *et al*., 2003; Rahman *et al*., 2010; Hossain *et al*., 2011).

In this paper, a hybrid air-cushion vehicle defined as semi-track air-cushion vehicle (STACV) is proposed and a prototype has been developed (Figure 1). The STACV is composed of two subsystems, i.e., the semi-tracks for propulsion, and the air-cushion to partially lift the vehicle. By introducing an adjustable suspension-like spring linkage between the propulsion system and the lifting system, the relative height from vehicle body to ground can be adjusted by controlling air-cushion pressure. And the loads respectively supported by tracks and cushion can also be controlled to adjust the track load in order to adapt different terrain surfaces. A properly-designed valve system (Figure 2) can be used to re-distribute air lift forces within the concerned area to further control the vehicle body attitude.

Meanwhile, a hierarchy controller is designed for the following purposes,

(1) To minimize the total power consumption by using the proposed hybrid generalized extremal optimization (HGEO) algorithm (Xie *et al*., 2009);
(2) To reduce the effect of both system nonlinearity and parametric uncertainty in order to follow the driver's commands and maintain the body horizontal attitude better by using the model predictive control (MPC) (Lee and Ricker, 1994);
(3) To assign the target driving torques and the target air-cushion pressures by using sequential quadratic programming (SQP) method;
(4) To realize the target driving torques and the target air-cushion pressures by using an air-cushion inverse neural network model and a PID controller.

2. VEHICLE MODEL

In order to design controller, the whole vehicle model, including air-cushion system characteristic model and dynamics model, are established.

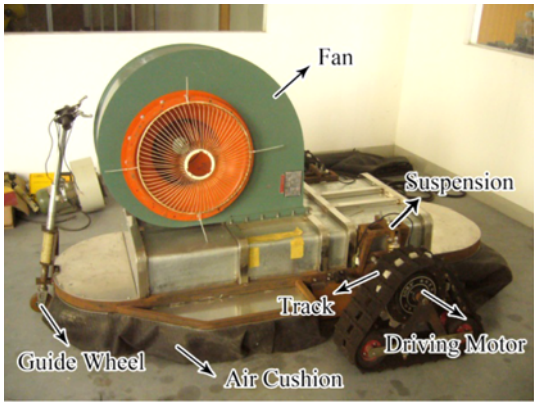

Figure 1. A prototype of STACV.

**Corresponding author*: e-mail: fanyu@sjtu.edu.cn

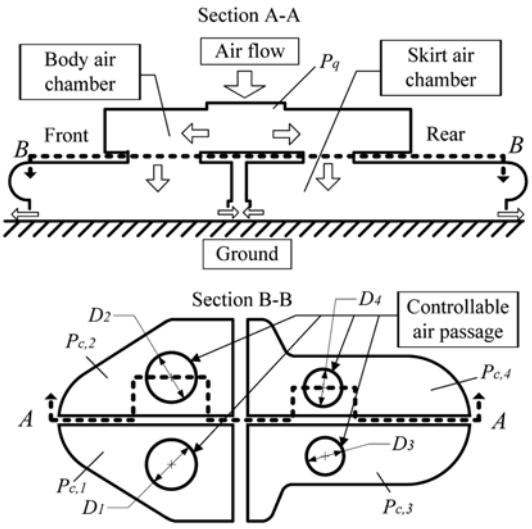

Figure 2. Controllable valve system.

2.1. Air-cushion System Characteristic Model

The valve system of air-cushion is designed as shown in Figure 2.

The high-pressure air, generated by the centrifugal fan, flows into body air chamber firstly; then, it is separated into four parts when passing through four controllable air passages; finally, it leaks out from the gap between the air-cushion skirt and the ground.

In previous research (Bekker, 1969; Wong, 2001), the corresponding volume flow rate Q_j is given by

$$Q_j = h_{c,j} l_{c,j} D_{c,j} \sqrt{2P_{c,j}/\rho_j} \qquad (j = 1\sim4) \tag{1}$$

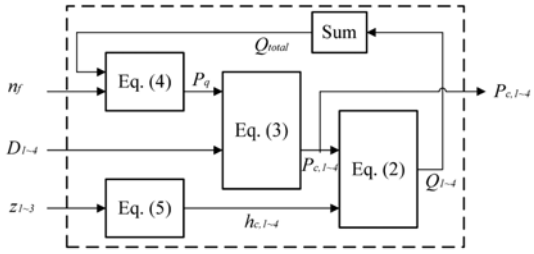

Figure 3. Neural network model of air-cushion system.

In which, $h_{c,j}$ is the corresponding air-cushion clearance height; $l_{c,j}$ is the corresponding air-cushion perimeter; $D_{c,j}$ is the corresponding discharge coefficient; $P_{c,j}$ is the air-pressure of corresponding skirt air chamber; ρ_j is the density of air inside corresponding skirt air chamber.

According to the fixed structure and geometry of the prototype, $l_{c,j}$ and $D_{c,j}$ have certain relationships with $h_{c,j}$. And also ρ_j has a certain relationship with $P_{c,j}$. Thus equation (1) can be rewritten as

$$Q_j = f_j(h_{c,j}, P_{c,j}) \qquad (j = 1\sim4) \tag{2}$$

Where f_j represents the mapping relationship among $h_{c,j}$, $P_{c,j}$ and Q_j.

Meanwhile, $P_{c,j}$ can be determined by the fan inlet total pressure Pq and diameters of four air passage D_j.

Thus the relationship can be expressed as,

$$[P_{c,1}, P_{c,2}, P_{c,3}, P_{c,4}]^T = g([P_q, D_1, D_2, D_3, D_4]^T) \tag{3}$$

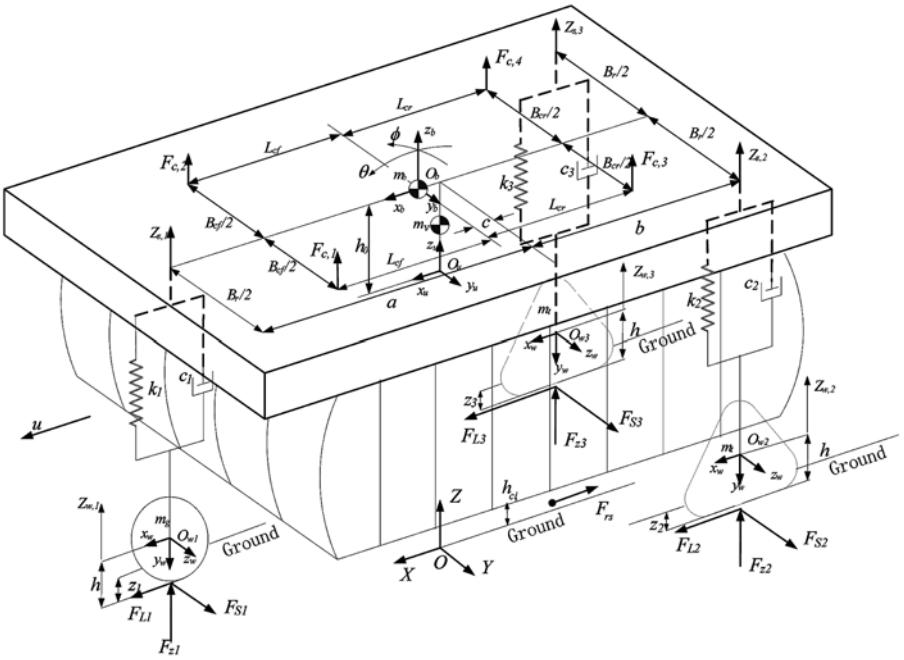

Figure 4. Modeling variables of the STACV.

Where g represents the mapping relationship between vector $[P_{c,1}, P_{c,2}, P_{c,3}, P_{c,4}]^{\mathrm{T}}$ and vector $[P_q, D_1, D_2, D_3, D_4]^{\mathrm{T}}$.

In additional, fan characteristic equation (Anderson, 2001) and relationships between $h_{c,j}$ and sinkage z_i are introduced in equations (4) and (5) respectively.

$$P_q = h(Q_{total}, n_f) \tag{4}$$

$$[h_{c,1}, h_{c,2}, h_{c,3}, h_{c,4}]^T = G([z_1, z_2, z_3]^T) \tag{5}$$

where Q_{total} is the total volume flow rate; n_f is rotational speed of fan; h represents mapping relationship among Pq, Q_{total} and n_f. G represents mapping relationship between vector $[h_{c,1}, h_{c,2}, h_{c,3}, h_{c,4}]^{\mathrm{T}}$ and vector $[z_1, z_2, z_3]^{\mathrm{T}}$.

The relationship of all related variables can be expressed in Figure 3.

By ignoring the detailed structure and the specific expressions of equations inside the dashed box, a neural network model can be introduced to replace the whole model inside dashed box, with 8 inputs n_f, $D_{1\sim4}$, $z_{1\sim3}$ and 4 outputs $P_{c,1\sim4}$.

The network is trained by the relevant input and output data which is gathered from a series of related tests in previous study (Xie *et al*., 2012). It is used as reference model in control algorithm design.

2.2. Vehicle Dynamics Model

Theoretically, a simplified vehicle model with 8 degree of freedom (longitudinal, lateral, yaw, roll, pitch and vehicle body bounce) is established in equation (6) and the involved variables are shown in Figures 4 and 5 in detail.

In equation (6), $k_1 = k_{sf}$, where k_{sf} is the front suspension stiffness; $k_{2,3} = k_{sr}/2$, where k_{sr} is the rear suspension stiffness; $c_1 = c_{sf}$, where c_{sf} is the damping coefficient of front suspension; $c_{2,3} = c_{sr}/2$, where c_{sr} is the damping coefficient of rear suspension; the vehicle roll stiffness $k_\varphi = k_{sr}B_r^2/4$, where B_r is the distance between the geometric centers of the rear semi-tracks; the vehicle roll damping coefficient $c_\varphi = c_{sr}B_r^2/4$; the vehicle pitch stiffness $k_\theta = k_{sf}(\mathrm{a}-\mathrm{c})^2 + k_{sr}(\mathrm{b}+\mathrm{c})^2$.

In equation (6), the vehicle pitch damping coefficient $c_\theta = c_{sf}(\mathrm{a}-\mathrm{c})^2 + c_{sr}(\mathrm{b}+\mathrm{c})^2$; B_{cf} and B_{cr} are the front and rear lateral distances between left and right air force equivalent action points respectively; L_{cf} and L_{cr} are the longitudinal distances from front and rear air-cushion force acting points to vehicle body geometric center respectively; the front guide wheel and rear semi-track sinkages are defined as the inverse of the vertical wheel displacement, $z_i = z_{w,i}$, $i = 1 \sim 3$; $F_{c,j}$ are air-cushion forces, $F_{c,j} = P_{c,j}S_{c,j}$, $j = 1 \sim 4$ where $S_{c,j}$ is equivalent projected area of corresponding skirt air chamber; $F_{stat,z1}$, $F_{stat,z2}$ and $F_{stat,z3}$ are the vertical ground support forces at initial time, defined as follows,

$$\begin{cases} F_{stat,z1} = m_g g + m_b g\dfrac{b+c}{a+b} \\ F_{stat,z2} = F_{stat,z3} = m_t g + \dfrac{1}{2}m_b g\dfrac{a-c}{a+b} \end{cases} \tag{7}$$

F_x, F_y and M_z are the total longitudinal, lateral forces and yaw moment respectively. The expressions are shown as follows,

$$\begin{cases} F_x = F_{L1}\cos\delta_D - F_{S1}\sin\delta_D + F_{L2} + F_{L3} - F_{rs}\cos\beta_b \\ F_y = F_{L1}\sin\delta_D + F_{S1}\cos\delta_D + F_{S2} + F_{S3} - F_{rs}\sin\beta_b \\ M_z = (F_{L3} - F_{L2})\dfrac{B_r}{2} - (F_{S2} + F_{S3})b \\ \qquad\quad + (F_{L1}\sin\delta_D + F_{S1}\cos\delta_D)a \end{cases} \tag{8}$$

where β_b is the vehicle body slip angle, defined as,

$$\beta_b = \tan^{-1}\left(\frac{v - h_0\dot{\phi} + c\dot{\psi}}{u + h_0\dot{\theta}}\right) \tag{9}$$

$$\begin{cases} m_v(\dot{u} - v\dot{\psi}) + m_b h_0(\ddot{\theta} + \dot{\phi}\dot{\psi}) = F_x \\ m_v(\dot{v} + u\dot{\psi}) + m_b h_0(\dot{\theta}\dot{\psi} - \ddot{\phi}) = F_y \\ I_{zz}\ddot{\psi} - I_{xz}\ddot{\phi} = M_z \\ I_{b,xx}\ddot{\phi} - I_{b,xz}\ddot{\psi} = m_b h_0(\dot{v} + u\dot{\psi} + h_0\dot{\theta}\dot{\psi} - h_0\ddot{\phi} + c\dot{\psi}) - (k_\varphi - m_b g h_0)\phi - c_\varphi\dot{\phi} \\ \qquad + \dfrac{k_{sr}}{2}(z_{w,2} - z_{w,3})\dfrac{B_r}{2} + \dfrac{c_{sr}}{2}(\dot{z}_{w,2} - \dot{z}_{w,3})\dfrac{B_r}{2} + (F_{c,1} - F_{c,2})\dfrac{B_{cf}}{2} + (F_{c,3} - F_{c,4})\dfrac{B_{cr}}{2} \\ I_{b,yy}\ddot{\theta} = m_b h_0(\dot{u} - v\dot{\psi} + h_0\dot{\phi}\dot{\psi} - c\dot{\psi}^2 + h_0\ddot{\theta}) - m_b c(\ddot{z}_b - c\ddot{\theta}) - k_\theta\theta - c_\theta\dot{\theta} - [k_{sr}(b+c) - k_{sf}(a-c)]z_b - [c_{sr}(b+c) - c_{sf}(a-c)]\dot{z}_b \\ \qquad - k_{sf}z_{w,1}(a-c) - c_{sf}\dot{z}_{w,1}(a-c) + \dfrac{k_{sr}}{2}(z_{w,2} + z_{w,3})(b+c) + \dfrac{c_{sr}}{2}(\dot{z}_{w,2} + \dot{z}_{w,3})(b+c) - (F_{c,1} + F_{c,2})L_{cf} + (F_{c,3} + F_{c,4})L_{cr} \\ m_b\ddot{z}_b = -(k_{sf} + k_{sr})z_b - (c_{sf} + c_{sr})\dot{z}_b - [k_{sr}(b+c) - k_{sf}(a-c)]\theta - [c_{sr}(b+c) - c_{sf}(a-c)]\dot{\theta} + \sum_{i=1}^{3}k_i z_{w,i} + \sum_{i=1}^{3}c_i\dot{z}_{w,i} + \sum_{j=1}^{4}F_{c,j} \\ m_g\ddot{z}_{w,1} = k_{sf}[z_b - (a-c)\theta - z_{w,1}] + c_{sf}[\dot{z}_b - (a-c)\dot{\theta} - \dot{z}_{w,1}] - k_{soil,f}|z_{w,1}|^{\frac{2n+1}{2}} - c_{soil,f}\dot{z}_{w,1} + F_{stat,z1} \\ m_t\ddot{z}_{w,2} = \dfrac{k_{sr}}{2}[z_b + (b+c)\theta + \dfrac{B_r}{2}\phi - z_{w,2}] + \dfrac{c_{sr}}{2}[\dot{z}_b + (b+c)\dot{\theta} + \dfrac{B_r}{2}\dot{\phi} - \dot{z}_{w,2}] - k_{soil,r}|z_{w,2}|^n - c_{soil,r}\dot{z}_{w,2} + F_{stat,z2} \\ m_t\ddot{z}_{w,3} = \dfrac{k_{sr}}{2}[z_b + (b+c)\theta - \dfrac{B_r}{2}\phi - z_{w,3}] + \dfrac{c_{sr}}{2}[\dot{z}_b + (b+c)\dot{\theta} - \dfrac{B_r}{2}\dot{\phi} - \dot{z}_{w,3}] - k_{soil,r}|z_{w,3}|^n - c_{soil,r}\dot{z}_{w,3} + F_{stat,z3} \\ I_{wz,i}\dot{\omega}_i = T_i - F_{t,Li}\cdot r_{eff,i} \quad (i = 1\sim3,\ T_1 = 0) \end{cases} \tag{6}$$

F_{rs} is the skirt-ground contact resistance as follows,

$$F_{rs} = C_{sk}\sum_{j=1}^{4} F_{c,j} \tag{10}$$

Where C_{sk} is the coefficient of skirt contact resistance.

In equation (11), the longitudinal and lateral forces of the front guide wheel and rear semi-tracks are approximated as follows,

$$\begin{cases} F_{Li} = F_{t,Li} - F_{rc,Li} - F_{rb,Li} \\ F_{Si} = (F_{t,Si} - F_{rc,Si} - F_{rb,Si})\mathrm{STEP}(\alpha_i, -10, -1, 10, 1) \end{cases} \quad (i = 1\sim3) \tag{11}$$

The expression of the STEP function can be given as follows,

$$\mathrm{STEP}(\alpha,\ \alpha_{lower},\ H_{lower},\ \alpha_{upper},\ H_{upper}) = \begin{cases} H_{lower} & \alpha \le \alpha_{lower} \\ H_{lower} + a_m\Delta^2(3-2\Delta) & \alpha_{lower} < \alpha < \alpha_{upp} \\ H_{upper} & \alpha \ge \alpha_{upper} \end{cases} \tag{12}$$

Where α is the wheel slip angle; α_{lower} and α_{upper} are lower and upper bounds of the slip angle respectively; H_{lower} and H_{upper} are the lower and upper bounds of STEP function respectively; a_m is the step height, $a_m = H_{upper}\ H_{lower}$; and $\Delta = (\alpha-\alpha_{lower}) / (\alpha_{upper}-\alpha_{lower})$.

In equation (11), $F_{rc,Li}$, and $F_{rc,Si}$ are the soil compaction resistance of propelling system in longitudinal and lateral directions. Using the empirical formula (Bekker, 1969), they can be expressed in following forms,

$$\begin{cases} F_{rc,L1} = k_{rcf,L} z_1^{n+1} \\ F_{rc,Li} = k_{rcr,L} z_1^{n+1} \\ F_{rc,S1} = k_{rcf,S} z_1^{n+1} \\ F_{rc,Si} = k_{rcr,S} z_1^{n+1} \end{cases} \quad (i = 2\sim3) \tag{13}$$

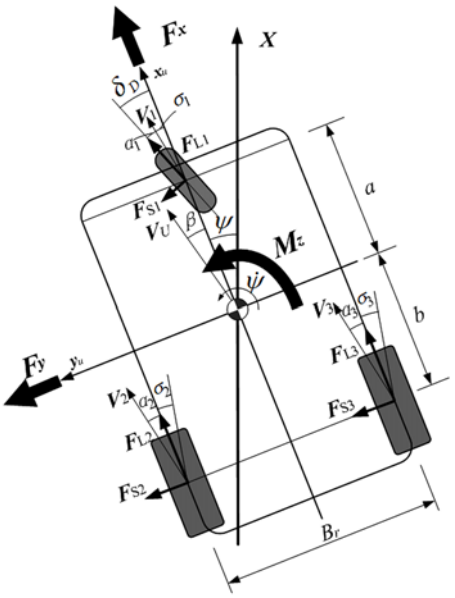

Figure 5. Other modeling variables of the STACV.

Where the related coefficients are defined as,

$$\begin{aligned} k_{rcf,L} &= \frac{k_c + B_g k_\varphi}{n+1} \qquad k_{rcf,S} \approx \frac{k_c + 0.5Dk_\varphi}{n+1} \\ k_{rcr,L} &= \frac{k_c + B_t k_\varphi}{n+1} \qquad k_{rcr,S} = \frac{k_c + L_t k_\varphi}{n+1} \end{aligned} \tag{14}$$

Where B_g is the width of front guide wheel; B_t is the width of rear semi-track; D is the diameter of the front guide wheel; L_t is the length of the semi-track; the related terrain parameters k_c, k_φ and n are the cohesive modulus of terrain deformation, frictional modulus of terrain deformation and exponent of soil deformation respectively.

On soft terrain surface or loose soils, the soil bulldozing resistance of propelling system can be expressed in the following forms according to the empirical formula from Bekker,

$$\begin{cases} F_{rb,L1} = k_{rbf,L1} z_1 + k_{rbf,L2} z_1^2 \\ F_{rb,Li} = k_{rbr,L1} z_i + k_{rbr,L2} z_i^2 \qquad (i = 2, 3) \\ F_{rb,S1} = k_{rbf,S1} z_1 + k_{rbf,S2} z_1^2 \\ F_{rb,Si} = k_{rbr,S1} z_i + k_{rbr,S2} z_i^2 \qquad (i = 2, 3) \end{cases} \tag{15}$$

Where the coefficients can be obtained by

$$\begin{aligned} &k_{rbf,L1} = 0.67 B_g c_s K'_{pc} \quad k_{rbf,L2} = 0.5 B_g \gamma_s K'_{p\gamma} \\ &k_{rbf,S1} \approx 0.67 \frac{D}{2} c_s K'_{pc} \quad k_{rbf,S2} \approx 0.5 \frac{D}{2} \gamma_s K'_{p\gamma} \\ &k_{rbr,L1} = 0.67 B_t c_s K'_{pc} \quad k_{rbr,L2} = 0.5 B_t \gamma_s K'_{p\gamma} \\ &k_{rbr,S1} = 0.67 L_t c_s K'_{pc} \quad k_{rbr,S2} = 0.5 L_t \gamma_s K'_{p\gamma} \\ &K'_{pc} = (N'_c - \tan\varphi')\cos^2\varphi' \\ &\tan\varphi' = 2\tan\varphi / 3 \\ &K'_{p\gamma} = (2N'_\gamma / \tan\varphi' + 1)\cos^2\varphi' \end{aligned} \tag{16}$$

In which φ, c_s and γ_s are the angle of internal shearing resistance of the soil, the cohesion of soil and the weight density of the terrain respectively.

The tractive efforts that semi-tracks can get from terrain can be predicted by following equations,

$$\begin{cases} F_{t,L1} = 0 \\ F_{t,S1} = 0 \\ F_{t,Li} = \mathrm{sgn}(s_{Li})(A_t c_s + F_{zi}\tan\varphi) \times \{1 - \frac{K_s}{|s_{Li}|L_t}[1 - \exp(-\frac{|s_{Li}|L_t}{K_s})]\} \\ F_{t,Si} = \mathrm{sgn}(s_{Si})(A_t c_s + F_{zi}\tan\varphi) \times \{1 - \frac{K_s}{|s_{Si}|L_t}[1 - \exp(-\frac{|s_{Si}|L_t}{K_s})]\} \end{cases} \quad (i = 2,3) \tag{17}$$

Where A_t is the area of one semi-track in contact with terrain. The vertical support forces F_{zi} that one semi-track can get from terrain are modified by adding damping coefficient (Solis and Longoria, 2008), and they can be expressed with the front vertical support forces in the following forms,

$$\begin{cases} F_{z1} = k_{soil,f} z_1^{\frac{2n+1}{2}} + c_{soil,f} \dot{z}_1 \\ F_{z2} = k_{soil,r} z_2^{n} + c_{soil,r} \dot{z}_2 \\ F_{z3} = k_{soil,r} z_3^{n} + c_{soil,r} \dot{z}_3 \end{cases} \tag{18}$$

Where the related terrain stiffness can be expressed as,

$$\begin{cases} k_{soil,f} = (1-n/3)(k_c + B_g k_\varphi)\sqrt{D} \\ k_{soil,r} = (k_c + B_i k_\varphi) L_t \qquad (i = 2, 3) \end{cases} \tag{19}$$

In equation (19), the related terrain damping coefficients $c_{soil,f}$, $c_{soil,r}$ can be got from experiments. The longitudinal and lateral semi-track slip rates are defined in the wheel center plane and the direction is perpendicular to it, which is different from Burckhardt approach (Kiencke and Nielsen, 2000), and can be given as follows,

$$s_{Li} = \begin{cases} \dfrac{r_{eff}\omega_i - V_i \cos\alpha_i}{V_i \cos\alpha_i} \\ \qquad r_{eff}\omega_i \le V_i \cos\alpha_i \text{(braking)} \\ \dfrac{r_{eff}\omega_i - V_i \cos\alpha_i}{r_{eff}\omega_i} \\ \qquad r_{eff}\omega_i > V_i \cos\alpha_i \text{(driving)} \end{cases} \qquad (i = 2,3) \tag{20}$$

$$s_{Si} = \begin{cases} (1+s_{Li})\tan\alpha_i \\ \qquad r_{eff}\omega_i \le V_i \cos\alpha_i \text{(braking)} \\ \tan\alpha_i \\ \qquad r_{eff}\omega_i > V_i \cos\alpha_i \text{(driving)} \end{cases} \qquad (i = 2,3) \tag{21}$$

Where r_{eff} is the effective turning radius of rear semi-track; ω_i is the turning speed of semi-track drive motor, V_i is the velocity of corresponding semi-track, and the related force projection angles are defined as follows,

$$\begin{cases} \sigma_1 = \sigma_f = \tan^{-1}\left(\dfrac{v + a\dot{\psi}}{u}\right) \\ \sigma_2 = \sigma_3 = \sigma_r = \tan^{-1}\left(\dfrac{v - b\dot{\psi}}{u}\right) \end{cases} \tag{22}$$

The front guide wheel and semi-track slip angle α can be estimated as,

$$\alpha = \begin{cases} \delta_D - \sigma_f & \text{(Front guide wheel)} \\ -\sigma_r & \text{(Rear semi-tracks)} \end{cases} \tag{23}$$

After substituting soil compaction resistances, soil bulldozing resistances and tractive efforts, the longitudinal and lateral forces of the front guide wheel and rear semi-tracks can be acquired.

3. CONTROLLER DESIGN

3.1. Main Control Strategy

The overall control framework is shown in figure 6. The optimal power consumption module calculates the vehicle target motion forces and moments. It should not only follow the driver command but also minimize the total power consumption. The feedback controller module deals with the compensation based on the measured vehicle motion variables. The generalized force distribution module focuses on realization of the target motion forces and moments by distributing them to air-cushion and semi-track. And finally, a air-cushion system inverse characteristic model is used to realize the desired air-cushion pressures and a PID controller is used to maintain the slip ratio of the semi-track. Each module will be introduced in the following sub-sections.

3.2. Optimal Power Consumption Module

According to previous researches, main energy consumption of STACV composes of two parts, to form and maintain the air-cushion to support the vehicle and to drive the propulsive mechanisms to overcome travelling resistances respectively (Wong, 2001). For the STACV concerned in this paper, the suitable load distribution ratio between the air-cushion system and propelling system is selected in order to minimize the total power consumption. It is based on vehicle's quasi-steady-state conditions.The power consumption model can be expressed as,

$$N = N_c + N_q \tag{24}$$

where N_c is the basic power consumed by air-cushion system and N_q is the power consumed by propelling system. N_c is given by,

$$N_c = \sum_{j=1}^{4} P_{c,j} Q_j \tag{25}$$

For the propelling system, the power is mainly consumed by driving demand. Here we only consider the longitudinal directional part, as it makes up the main part of the energy consumption. It is given by,

$$N_q = (F_{t,L2} + F_{t,L3})u \tag{26}$$

Where u is the longitudinal speed of the vehicle.

Combining equations (2), (17) and (26) and assuming S_{S2}, S_{S3} to be zero, total power consumption of the vehicle is determined by the only 6 variables, i.e. $P_{c,1\sim4}$, S_{L2}, S_{L3}.

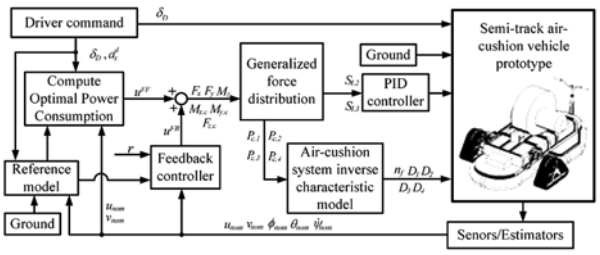

Figure 6. Control frame of STACV.

The constraints can be summarized as follows,

(1) The front guide wheel and the rear semi-tracks must touch the ground;
(2) The driving forces must accord with the acceleration;
(3) The sinkage difference among wheels or semi-tracks should be as small as it can be;
(4) The related air-cushion pressures and slip rates are within the applicable range;

A new stochastic method named hybrid generalized extremal optimization (HGEO), which combines genetic algorithm (GA) and generalized extremal optimization (GEO), is introduced to search optimal point. It has been proved that HGEO has better performance than GAs or other related simpler algorithms proposed in previous study (Xie *et al*., 2009).

After the optimal process, the desired generalized vehicle motion forces given by equation (27), including longitudinal force F_{x_FF}, lateral force F_{y_FF}, yaw moment M_{z_FF}, the roll torque $M_{x\_FF,c}$ pitch torque $M_{y\_FF,c}$, and total air-cushion vertical force $F_{z\_FF,c}$, can be provided by equation (28) according to equation (6).

$$u^{FF} = [F_{x\_FF} F_{y\_FF} M_{z\_FF} M_{x\_FF,c} M_{y\_FF,c} F_{z\_FF,c}]^T \tag{27}$$

$$\begin{cases} F_{x\_FF} = m_v a_{x,d} \\ F_{y\_FF} = m_v u_{nom} \dot{\psi}_d \\ M_{z\_FF} = 0 \\ M_{x\_FF,c} = (F_{c\_FF,1} - F_{c\_FF,2}) \dfrac{B_{cf}}{2} \\ \qquad\qquad + (F_{c\_FF,3} - F_{c\_FF,4}) \dfrac{B_{cr}}{2} \\ M_{y\_FF,c} = -(F_{c\_FF,1} + F_{c\_FF,2}) L_{cf} \\ \qquad\qquad + (F_{c\_FF,3} + F_{c\_FF,4}) L_{cr} \\ F_{z\_FF,c} = \sum_{j=1}^{4} F_{c\_FF,j} \end{cases} \tag{28}$$

In equation (28), $a_{x,d}$ is the target longitudinal acceleration acquired from driver command; $\dot{\psi}_d$ is target yaw rate determined by (Shen and Yu, 2007),

$$\dot{\psi}_d = \frac{1}{1 + K_d [u_{nom}^2 / (B_r \cdot g)]} \frac{u_{nom}}{B_r} \delta_D \tag{29}$$

Where K_d is ideal understeer characteristics; u_{nom} is nominal longitudinal velocity acquired from sensors; g is the gravitational acceleration; δ_D is the steering angle of the guide wheel.

In equation (28), $F_{c\_FF,1\sim4}$ are the corresponding air-cushion forces with expressions $F_{c\_FF,j} = P_{c\_FF,j} S_{c,j}$, where $P_{c\_FF,j}$ are the solutions of optimal problem.

From the equation (28), we can see that the optimal power consumption module can provide the control objectives, i.e. generalized vehicle motion forces, to keep the vehicle states close to the desired running states. The deviation and unconsidered dynamics will be handled by the feedback control module.

3.3. Model Predictive Feedback Control Module

STACV and its operation environment, i.e. soft terrain, are both complex nonlinear time-varying systems. The precise reference model needed by common controllers cannot be established due to system nonlinearity and parametric uncertainty.

The feedback controller is designed using the Model Predictive Control (MPC) method (Lee and Ricker, 1994), and the general control structure of which is shown in figure 7.

Work principle of MPC is described as follows,

(1) Establish the current prediction model according to a non-parametric prediction model and system status at k time;
(2) Solve the optimization problems and get the sequence of control signal according to obtain current prediction model;
(3) Use the first step of control sequences to control the object;
(4) Obtain another current prediction model at k+1 time.

To design the feedback controller, the prediction model is obtained after linearization of equation (6) on nominal working point, which has the following form,

$$\begin{cases} \dot{X} = AX + Bu^{FB} \\ Y = CX \end{cases} \tag{30}$$

Where $A \in R^{15\times15}$, $B \in R^{15\times6}$, $C \in R^{5\times15}$ are the corresponding state space matrices. The state vector X is defined as follows,

$$X = [\Delta u\ \Delta v\ \Delta\phi\ \Delta\dot{\phi}\ \Delta\theta\ \Delta\dot{\theta}\ \Delta\dot{\psi}\ \Delta z_b\ \Delta\dot{z}_b\ \Delta z_{w,1}\ \Delta z_{w,2}\ \Delta z_{w,3}\ \Delta\dot{z}_{w,1}\ \Delta\dot{z}_{w,2}\ \Delta\dot{z}_{w,3}]^T \tag{31}$$

In which 'Δ' denotes the relative value with respect to nominal working point. The control outputs u^{FB} are defined as,

$$u^{FB} = [F_{x\_FB}\ F_{y\_FB}\ M_{z\_FB}\ M_{x\_FB,c}\ M_{y\_FB,c}\ F_{z\_FB,c}]^T \tag{32}$$

To adjust the vehicle body attitude, the feedback controller will re-distribute the air-cushion moment. To simplify the problem, the total vertical air-cushion forces are assumed to be only selected by optimal power consumption module, so the feedback part of the vertical

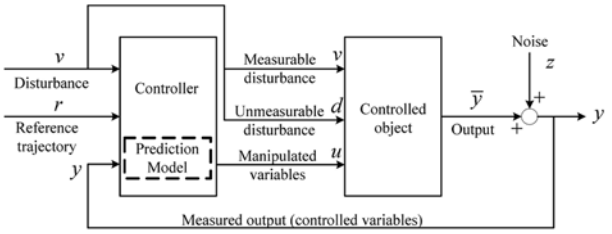

Figure 7. Scheme of model predictive control.

air-cushion force is set to be zero, i.e. $F_{z\_FB,c}$=0.

The inputs are vehicle longitudinal velocity, lateral velocity, roll angle, pitch angle and yaw rate, which can be expressed as,

$$Y=[\Delta u \quad \Delta v \quad \Delta\phi \quad \Delta\theta \quad \Delta\dot{\psi}]^T \tag{33}$$

The reference vector r contains the desired reference states for the feedback loop, which is defined as,

$$r=\begin{bmatrix} u_d & v_d & \phi_d & \theta_d & \dot{\psi}_d \end{bmatrix}^T \tag{34}$$

where u_d, v_d, φ_d and θ_d are the desired reference longitudinal velocity, lateral velocity, pitch angle and roll angle respectively.

In practical situations, the desired reference longitudinal velocity is determined by driver command; according to previous study and comfort requirements, lateral velocity, roll angle and pitch angle should be restrained to near zero; yaw rate should be maintained at a certain value, which is given by equation (29). So the desired reference states should be,

$$r^d=[u_0+a_{x,d}t \;\; 0 \;\; 0 \;\; 0 \;\; \frac{1}{1+K_d[u_{nom}^2/(B_r\cdot g)]}\frac{u_{nom}}{B_r}\delta_D]^T \tag{35}$$

The MPC action at k time is obtained by solving the constrained optimization problem. The cost function of MPC problem is shown in compact matrices form as follows,

$$\begin{aligned} \min\ & J(\Delta u,\varepsilon)=U^TW_u^2U+\Delta U^TW_{\Delta u}^2\Delta U \\ & +Y_k^TW_y^2Y_p+\rho_\varepsilon\varepsilon^2 \\ \text{s.t.}\ & \begin{bmatrix} Y_{k,\min} \\ U_{\min} \\ \Delta U_{\min} \end{bmatrix} \le \begin{bmatrix} Y_k \\ U \\ \Delta U \end{bmatrix} \le \begin{bmatrix} Y_{k,\max} \\ U_{\max} \\ \Delta U_{\max} \end{bmatrix} \end{aligned} \tag{36}$$

where U is the difference between the control variables and the target control variables vector with respect to the k step of the prediction horizon; ΔU is the control variables change rate with respect to the k step of the prediction horizon; Y_k is the difference between the controlled variables and reference vector; W_u, ΔW_u, W_y are the related nonnegative weighting matrices; ε is the slack variable, and ρ_ε is the weight on the slack variable; $Y_{k,min}$, U_{min}, ΔU_{min}, $Y_{k,max}$, U_{max}, ΔU_{max} are the bound constraints for Y_k, U and ΔU.

By minimizing $J(\Delta u,\varepsilon)$, Δu is derived by using the quadratic programming with constraints. Then new control variable $u(k)$ is gotten by just adding the obtained control input increments $\Delta u(k|k)$ to previews control input $u(k-1)$, i.e.,

$$u(k)=u(k-1)+\Delta u(k|k) \tag{37}$$

In which the control input increments $\Delta u(k|k)$ is the first element of the sequence of increments, which is obtained by optimized solutions.

$$\{\Delta u(k|k),\Delta u(k+1|k),\ldots\ldots\Delta u(m-1+k|k)\} \tag{38}$$

Thus the operation states can be maintained around the desired running target, which is the output of optimal power consumption module.

3.4. Generalized Force Disturbution Module

The above calculated forces and moments need to be converted to more specific physical variables, i.e. left and right semi-tracks longitudinal slip ratio S_{L2}, S_{L3}, and four air-cushion pressures $P_{c,1\sim4}$. The conversion mechanism has been achieved using a sequential quadratic programming approach (Hattori *et al*., 2002; Shen and Yu, 2007). The principal is to establish a dynamical trade-off between vehicle force tracking errors and the magnitudes of control inputs within wheel-terrain interaction limit.

First, a weighted cost function is specified to convert the original nonlinear constrained optimization problem to an unconstrained one as follows,

$$J_{SQP}=E^TW_EE+\Delta u_c^TW_{\Delta u_c}\Delta u_c+u_c^TW_{u_c}u_c \tag{39}$$

Where the error vector E is defined as differences between the desired and actual forces,

$$\begin{aligned} E&=u^*-u \\ &=[F_x^* \quad F_y^* \quad M_z^* \quad M_{x,c}^* \quad M_{y,c}^* \quad F_{z,c}^*]^T \\ &\quad -[F_x \quad F_y \quad M_z \quad M_{x,c} \quad M_{y,c} \quad F_{z,c}]^T \end{aligned} \tag{40}$$

Where

$$u^*=u^{FF}+u^{FB} \tag{41}$$

$$\Delta u_c=[\Delta s_{L2} \;\; \Delta s_{L3} \;\; \Delta P_{c,1} \;\; \Delta P_{c,2} \;\; \Delta P_{c,3} \;\; \Delta P_{c,4}]^T \tag{42}$$

$$u_c=[s_{L2} \quad s_{L3} \quad P_{c,1} \quad P_{c,2} \quad P_{c,3} \quad P_{c,4}]^T \tag{43}$$

W_E, $W_{\Delta uc}$ and W_{uc} are corresponding nonnegative weighting matrices. It is important to choose proper weighting matrices to achieve actuator limits and suitable convergence rate.

At the k +1 time,

$$u_c(k+1)=u_c(k)+\Delta u_c \tag{44}$$

$$u(k+1)\approx u(k)+J_{cob}\Delta u_c \tag{45}$$

Where J_{cob} is the transient Jacobian matrix, defined as $J_{cob}=\partial u/\partial u_c$. In each time step, the values of J_{cob} is determined by vehicle running parameters and feedback information from reference model.

Since the cost function J_{SQP} should be minimized with respect to the control input increments Δuc, the minimized cost function value is achieved when,

$$\partial J_{SQP}/\partial\Delta u_c=0 \tag{46}$$

The relations between vehicle motion forces u and propelling system & air-cushion forces $F_{t,c}$ can be rewritten as follows,

$$u = M_F F_{t,c} \tag{47}$$

Where

$$F_{t,c} = [F_{L1\sim3}, F_{S1\sim3}, F_{c1\sim4}] \tag{48}$$

In equation (47), transpose matrix M_F can be deduced by equations (8) and (28) as equation (49),

$$M_F = \begin{bmatrix} \cos\delta_D & 1 & 1 & -\sin\delta_D & 0 & 0 & -C_{sk}\cos\beta_b & -C_{sk}\cos\beta_b & -C_{sk}\cos\beta_b & -C_{sk}\cos\beta_b \\ \sin\delta_D & 0 & 0 & \cos\delta_D & 1 & 1 & -C_{sk}\sin\beta_b & -C_{sk}\sin\beta_b & -C_{sk}\sin\beta_b & -C_{sk}\sin\beta_b \\ a\sin\delta_D & -B_r/2 & B_r/2 & a\cos\delta_D & -b & -b & 0 & 0 & 0 & 0 \\ 0 & 0 & 0 & 0 & 0 & 0 & B_{qf}/2 & -B_{qf}/2 & B_{qr}/2 & -B_{qr}/2 \\ 0 & 0 & 0 & 0 & 0 & 0 & -L_{qf} & -L_{qf} & L_{qr} & L_{qr} \\ 0 & 0 & 0 & 0 & 0 & 0 & 1 & 1 & 1 & 1 \end{bmatrix} \tag{49}$$

So the final Jacobian matrix is

$$J_{cob} = \partial u/\partial u_c = M_F M_{JF} \tag{50}$$

Where

$$M_{JF} = \begin{bmatrix} \frac{\partial F_{L1}}{\partial s_{L2}} & \frac{\partial F_{L1}}{\partial s_{L3}} & \frac{\partial F_{L1}}{\partial P_{c,1}} & \frac{\partial F_{L1}}{\partial P_{c,2}} & \frac{\partial F_{L1}}{\partial P_{c,3}} & \frac{\partial F_{L1}}{\partial P_{c,4}} \\ \cdots & \cdots & \cdots & \cdots & \cdots & \cdots \\ \frac{\partial F_{L3}}{\partial s_{L2}} & \frac{\partial F_{L3}}{\partial s_{L3}} & \frac{\partial F_{L3}}{\partial P_{c,1}} & \cdots & \cdots & \frac{\partial F_{L3}}{\partial P_{c,4}} \\ \frac{\partial F_{S1}}{\partial s_{L2}} & \frac{\partial F_{S1}}{\partial s_{L3}} & \frac{\partial F_{S1}}{\partial P_{c,1}} & \frac{\partial F_{S1}}{\partial P_{c,2}} & \frac{\partial F_{S1}}{\partial P_{c,3}} & \frac{\partial F_{S1}}{\partial P_{c,4}} \\ \cdots & \cdots & \cdots & \cdots & \cdots & \cdots \\ \frac{\partial F_{S3}}{\partial s_{L2}} & \frac{\partial F_{S3}}{\partial s_{L3}} & \frac{\partial F_{S3}}{\partial P_{c,1}} & \cdots & \cdots & \frac{\partial F_{S3}}{\partial P_{c,4}} \\ \frac{\partial F_{c,1}}{\partial s_{L2}} & \frac{\partial F_{c,1}}{\partial s_{L3}} & \frac{\partial F_{c,1}}{\partial P_{c,1}} & \frac{\partial F_{c,1}}{\partial P_{c,2}} & \frac{\partial F_{c,1}}{\partial P_{c,3}} & \frac{\partial F_{c,1}}{\partial P_{c,4}} \\ \cdots & \cdots & \cdots & \cdots & \cdots & \cdots \\ \cdots & \cdots & \cdots & \cdots & \cdots & \cdots \\ \frac{\partial F_{c,4}}{\partial s_{L2}} & \frac{\partial F_{c,4}}{\partial s_{L3}} & \frac{\partial F_{c,4}}{\partial P_{c,1}} & \frac{\partial F_{c,4}}{\partial P_{c,2}} & \frac{\partial F_{c,4}}{\partial P_{c,3}} & \frac{\partial F_{c,4}}{\partial P_{c,4}} \end{bmatrix} \tag{51}$$

By combining equations (39)~(51), the desired increments of control variables can be obtained as follows,

$$\Delta u_{c,d} = (W_{u_c} + W_{\Delta u_c} + J_{cob}^T W_E J_{cob})^{-1} \times [J_{cob}^T W_E E_u - W_{u_c} u_c(k)] \tag{52}$$

Where E_u is the tracking error, i.e.,

$$E_u = u^*(k) - u(k) \tag{53}$$

Finally, the obtained air-cushion pressures and longitudinal semi-track slip ratios are realized by air-cushion system inverse characteristic model and the PID controller.

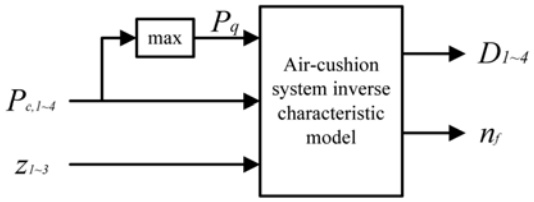

Figure 8. Scheme of Air-cushion system inverse characteristic model.

3.5. Air-Cushion System Inverse Characteristic Model

Air-cushion system inverse characteristic model is used to transform desired air-cushion pressures into fan rotational speed and diameters of each air passages as shown in figure 8.

It can be seen in figure 8 that P_q is determined only by the maximum value among $P_{c,1\sim4}$ and the model is established by neural network training with the same data mentioned in section 2.1.

3.6. PID Controller

PID controller is designed to convert desired longitudinal semi-track slip ratios into motor torque of semi-track through the calculation method, (Van Zanten *et al.*, 1996)

$$T_i = F_{i,Li} \cdot r_{eff,i} + k_p(S_{Li,d} - S_{Li}) + k_i(S_{Li,d} - S_{Li})/s \quad (i = 2, 3) \tag{54}$$

Where k_p is proportional coefficient, k_i is integral coefficient, S_{Li} is current slip ratio.

4. EXPERIMENTS AND DISCUSSIONS

In order to examine the effectiveness of the controller, two typical experiments are carried out. The process and results are shown in this section. In all figures of this section, the blue solid line, dark dash line, red dot-dash line and green dot line represent state target, dynamics response under the proposed control algorithm (MPC), dynamics response under PID control algorithm (PID) and dynamics response under optimal control algorithm without feedback (OPT)

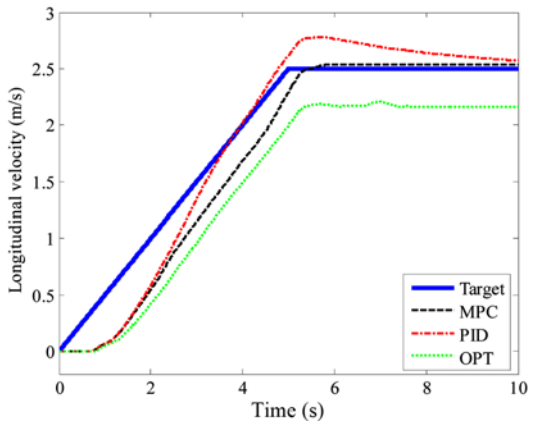

Figure 9. Longitudinal velocity of STACV.

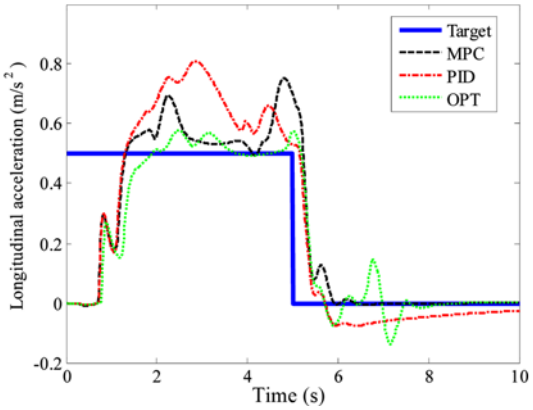

Figure 10. Longitudinal acceleration of STACV.

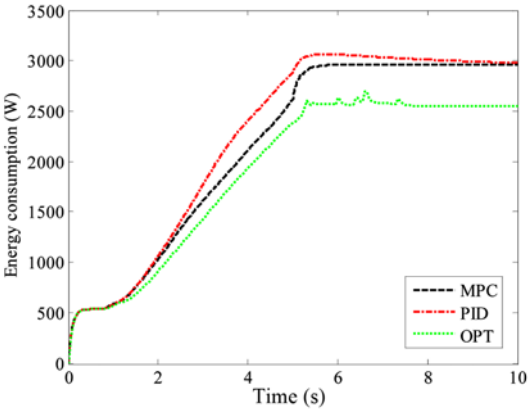

Figure 11. Energy consumption.

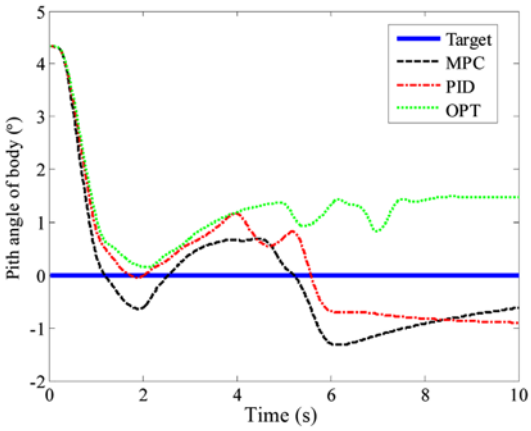

Figure 12. Pitch angle of body.

respectively.

4.1. Case 1: Acceleration on Soft Terrain

The STACV is desired to accelerate from 0 m/s to 2.5 m/s in 5 seconds and then to move forward uniformly. The dynamics response under the proposed control algorithm is recorded, comparing with other two control algorithms.

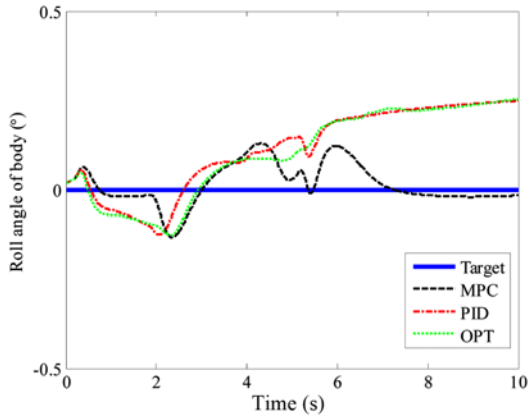

Figure 13. Roll angle of body.

In Figure 9, within time interval of 0 ~ 1s, the STACV doesn't move because of the low air-cushion lift forces. Comparing with other two control algorithm, the proposed controller gets closer to the state target.

The acceleration, energy consumption, pitch angle and roll angle of body are shown in Figures 10 ~ 13, which indicate that the proposed controller has better performance than other two controllers. Note that although optimal control algorithm has less energy consumption, it fails in following the desired longitudinal velocity.

4.2. Case 2: Joint Road

The STACV is desired to move from hard road surface into soft terrain surface at the third second with uniform speed of 1 m/s. Results are shown in Figure 14 ~ 18.

From the results it can be seen that when moving on hard road, the air-cushion system doesn't work and the propelling system undertakes whole weight load, which leads to lowest energy consumption; after entering the soft terrain, the fan starts to work, air-cushion system undertakes part of weight load.

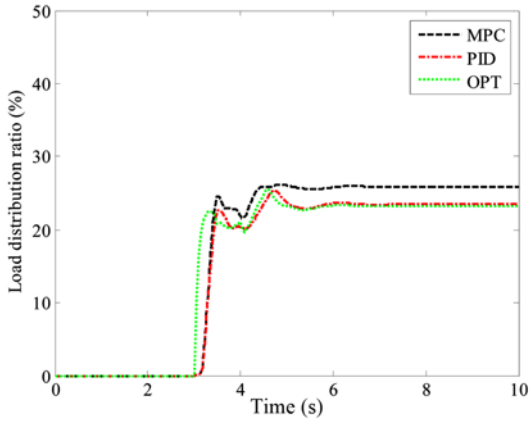

Figure 14. Load distribution ratio.

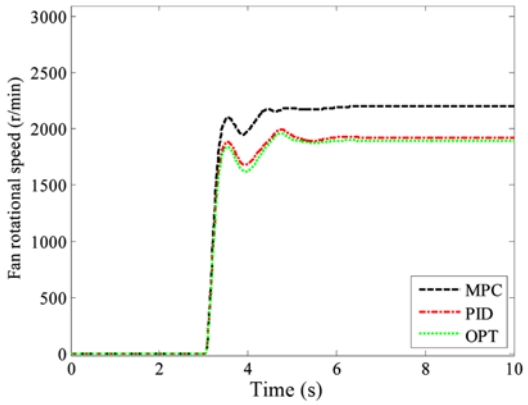

Figure 15. Fan rotational speed.

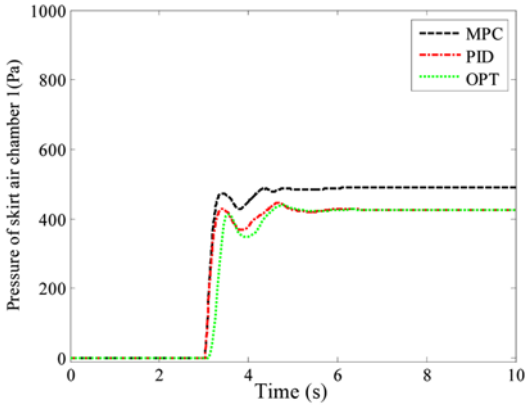

Figure 16. Pressure of skirt air chamber 1.

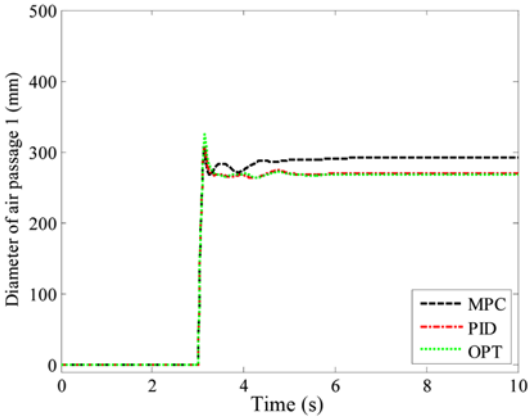

Figure 17. Diameter of air passage 1.

5. CONCULUSION

In this paper, a hybrid air-cushion vehicle is proposed. A reference dynamics model is established and air-cushion system neural network model is built, indicating the relationship among sinkages, fan rotational speed, diameters of air passages and air-cushion pressure.

The hierarchy controller using MPC algorithm, HGEO algorithm and PID controller has been established and its effectiveness has been verified by related experiments. The results show that the controller can maintain the body attitude properly, as well as lower the total energy consumption. Comparing with other control algorithms, the designed controller has better performance in following the target states by reducing the effect of both system nonlinearity and parametric uncertainty than that of other controllers proposed in previous work.

The paper has provided useful reference for soft-terrain vehicle and control system design and improved the trafficability of soft terrain vehicle.

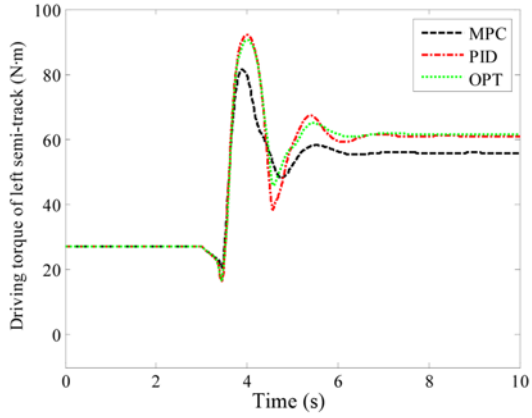

Figure 18. Driving torque of left semi-track.

ACKNOWLEDGEMENT–The research is sponsored by the Specialized Research Fund for the Doctoral Program of Higher Education of China under Grant No. 20100073110063 and National Natural Science Foundation of China under Grant No. 51375298.

REFERENCES

Anderson, J. D. (2001). *Fundamentals of Aerodynamics*. 2nd edn. McGraw-Hill. New York.

Bekker, M. G. (1969). *Introduction to Terrain-Vehicle Systems*. 1st edn. University of Michigan Press. Michigan.

Bertin, J. (1968). French air cushion vehicles developments. *Canadian Aeronautics and Space J.* **14**, **1**, 1–12.

Hattori, Y., Koibuchi, K. and Yokoyama, T. (2002). Force and moment control with nonlinear optimum distribution for vehicle dynamics. *Proc. 6th Int. Symp. Advanced Vehicle Control*, Hiroshima, Japan. 595–600.

Hossain, A., Rahman, A. and Mohiuddin, A. (2011). Cushion pressure control system for an intelligent air-cushion track vehicle. *J. Mechanical Science and Technology* **25**, **4**, 1035–1041.

Kiencke, U. and Nielsen, L. (2000). *Automotive Control Systems: For Engine, Driveline, and Vehicle*. 2nd edn.

Springer-Verlag. Berlin, Heidelberg.

Lee, J. H. and Ricker, N. L. (1994). Extended Kalman filter based nonlinear model predictive control. *Industrial & Engineering Chemistry Research* **33**, **6**, 1530–1541.

Luo, Z., Yu, F. and Chen, B. C. (2003). Design of a novel semi-tracked air-cushion vehicle for soft terrain. *Int. J. Vehicle Design* **31**, **1**, 112–123.

Rahman, A., Mohiuddin, A., Ismail, A., Yahya, A. and Hossain, A. (2010). Development of hybrid electrical air-cushion tracked vehicle for swamp peat. *J. Terramechanics* **47**, **1**, 45–54.

Shen, X. M. and Yu, F. (2007). Study on vehicle chassis control integration based on vehicle dynamics and separate loop design approach. *Int. J. Vehicle Autonomous Systems* **5**, **1**, 95–118.

Solis, J. M. and Longoria, R. G. (2008). Modeling track–terrain interaction for transient robotic vehicle maneuvers. *J. Terramechanics* **45**, **3**, 65–78.

Van Zanten, A. T., Erhardt, R., Pfaff, G., Kost, F., Hartmann, U. and Ehret, T. (1996). Control aspects of the Bosch-VDC. *Proc. 3rd Int. Symp. Advanced Vehicle Control*. Aachen, Germany. 573–608.

Wong, J. Y. (1973). On the application of air cushion technology to off-road transport. *Canadian Aeronautics and Space J.* **19**, **1**, 17–19.

Wong, J. Y. (2001). *Theory of Ground Vehicles*. 3rd edn. Wiley-Interscience. Ottawa.

Xie, D., Luo, Z. and Yu, F. (2009). The computing of the optimal power consumption for semi-track air-cushion vehicle using hybrid generalized extremal optimization. *Applied Mathematical Modelling* **33**, **6**, 2831–2844.

Xie, D., Ma, C. and Luo, Z. (2012). Research on air-cushion system test and simulation of semi-track air-cushion vehicle. *J. Mechanical Engineering* **48**, **4**, 120–128.